

# Energetics and Conformational Changes upon Complexation of a Phenothiazine Drug with Human Serum Albumin

Mohammad Arif Cheema,<sup>†</sup> Pablo Taboada,\* Silvia Barbosa, Emilio Castro,  
Mohammad Siddiq,<sup>‡</sup> and Víctor Mosquera

*Grupo de Física de Coloides y Polímeros, Departamento de Física de la Materia Condensada, Facultad de Física, Universidad de Santiago de Compostela, E-15782, Santiago de Compostela, Spain, and  
Department of Chemistry, Quaid-i-Azam University Islamabad, 45320, Pakistan*

*Received March 30, 2007; Revised Manuscript Received April 25, 2007*

The interactions and complexation process of the amphiphilic phenothiazine fluphenazine hydrochloride with human serum albumin in aqueous buffered solutions of pH 3.0 and 7.4 have been examined by  $\zeta$ -potential, isothermal titration calorimetry (ITC), UV–vis spectroscopy, and dynamic light scattering (DLS) techniques with the aim of analyzing the effect of hydrophobic and electrostatic forces on the complexation process and the alteration of protein conformation upon binding. Thus, the energetics and stoichiometry of the binding process were derived from ITC data. The enthalpies of binding obtained are small and exothermic, so the Gibbs energies of binding are dominated by large increases in entropy, consistent with hydrophobic interactions at a acidic pH. However, at physiological pH, binding to the first class of binding sites is dominated by an enthalpic contribution due to the existence of electrostatic interactions and probably some hydrogen bonding. Binding isotherms were obtained from microcalorimetric data by using a theoretical model based on the Langmuir isotherm.  $\zeta$ -Potential data showed a reversal in the sign of the protein charge at pH 7.4, as a consequence of the binding of the drug to the protein. Gibbs energies of drug binding per mole of drug were also derived from  $\zeta$ -potential data. On the other hand, binding of the phenothiazine that causes a conformational transition on the protein structure was followed as a function of drug concentration using UV–vis spectroscopy, and the data were analyzed to obtain the Gibbs energy of the transition in water ( $\Delta G_w^\circ$ ) and in a hydrophobic environment ( $\Delta G_{hc}^\circ$ ). Finally, the population distribution of the different species in solution and the size of the complexes were analyzed through dynamic light scattering. The existence of an aggregation process of drug/protein complexes, as a consequence of the expanded structure of the protein induced by the drug and subsequent further binding, is in agreement with ITC data. In addition, detection of drug aggregates at concentrations below the drug critical micelle concentration was also detected by this technique.

## Introduction

Human serum albumin (HSA) is the most abundant protein in blood plasma and serves as a depot and transport protein for numerous endogenous and exogenous compounds. Its principal function is to transport fatty acids, a great variety of metabolites, and drugs, such as anticoagulants, tranquilizers, and general anesthetics,<sup>1</sup> so it is considered as a model for studying drug–protein interactions in *in vitro*.<sup>2</sup> HSA is also the principal factor in contributing to the blood osmotic pressure and has been suggested as a possible source of amino acids for various tissues.<sup>3,4</sup> It consists of 585 amino acids with  $\sim 60\%$   $\alpha$ -helix and no  $\beta$ -strand with an asymmetric heart-shape with sides of 8 nm and a thickness of 3 nm.<sup>5</sup> The two heart “lobes” contain two binding sites, which consist almost exclusively of hydrophobic side chains, while the outside of the molecule contains most of the polar groups. The tip of the heart is positively charged at physiological pH. The globular structure is composed of three main domains that are loosely joined together through physical forces and six subdomains that are wrapped by disulfide bonds.

As commented above, many drugs, particularly those with local anesthetic, tranquilizer, antidepressant, and antibiotic actions, exert their activity by interaction with biological membranes. Thus, these drugs have to be carried to their sites

of action by means of protein carriers, as HSA, at which they bind with different affinities. Strong binding can decrease the concentration of free drug in plasma, whereas weak binding can lead to a low circulation time or poor distribution. In addition, it is important to realize that the pharmacokinetic function of HSA in participating in adsorption, distribution, metabolism, and excretion of drugs and other ligands can be well-governed by rare fluctuations into a particular subset of conformational substates, slightly different conformations within their native state (e.g., one where a gate is opened to admit a substrate to the active site), where the marginal stability of the native conformation is a delicate balance of diverse interactions such as electrostatic and van der Waals.<sup>6</sup> In particular, it is believed that the transport function of HSA is controlled through the N–B transition of this protein or akin to it,<sup>7–8</sup> which occurs between pH 7.0 and 9.0.<sup>3</sup> In addition, binding of ligands to the protein also induces conformational alterations in its native structure, altering this fragile equilibrium.<sup>3</sup> Therefore, analysis of the binding capacity and structure of the complexes between HSA and amphiphilic drugs are of particular interest in order to elucidate the means by which ligand affinity is regulated and how the protein conformation is altered upon complexation, since these factors play a key role in a vast range of important biochemical phenomena, for example, the reversible binding of oxygen by myoglobin.<sup>9</sup>

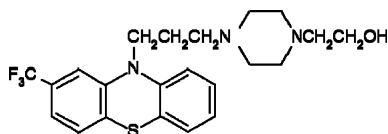
In the present work, we analyze the complexation process of the phenothiazine drug fluphenazine hydrochloride (see Scheme 1) to HSA in aqueous buffered solutions of pH 3.0, and 7.4,

\* To whom correspondence should be addressed. E-mail: fmpablo@usc.es.

<sup>†</sup> Permanent address: Department of Chemistry, Quaid-i-Azam University, Islamabad, 45320, Pakistan.

<sup>‡</sup> Quaid-i-Azam University.

Scheme 1



with a view to elucidate the effect of hydrophobic and electrostatic forces on the complexation process and the alteration of protein conformation upon binding. In recent reports, the self-aggregation process and the physicochemical properties of this drug have been studied.<sup>10–11</sup> The interest on phenothiazine drugs has increased over the last years since, apart from their use as tranquillizer-blocking dopamine receptors,<sup>12</sup> they have proved useful to fight against multidrug-resistant bacteria,<sup>13</sup> in the treatment of Creutzfeldt–Jacob disease,<sup>14</sup> as inhibitors of HIV-1 viral replication cycle,<sup>15</sup> as modulators of anticancer drug transport,<sup>16</sup> and as RNA scaffolds.<sup>17</sup>

Isothermal titration calorimetry measurements (ITC) were performed to determine the type and magnitude of the energies involved in the complexation process of this amphiphilic drug to HSA. The extent of drug adsorption was calculated using the theoretical model of Ueda and Yamanaka,<sup>18</sup> based on the Langmuir adsorption isotherm. The electrophoretic mobility of the HSA/phenothiazine complexes was measured, providing information on the adsorbed layer, the  $\zeta$ -potential of the complex, and the adsorption energies. UV–vis data were used to follow the conformational changes of the HSA structure upon binding and to calculate its free energy of unfolding. Finally, dynamic light scattering measurements were performed in order to characterize the complex size distributions.

## Experimental Section

**Materials.** Human serum albumin (70024-90-7) and fluphenazine hydrochloride {4-[3-[2-(trifluoromethyl)-10H-phenothiazin-10-yl]propyl]-1-piperazineethanol dihydrochloride} were obtained from Sigma Chemical Co. Protein was used after further purification by liquid chromatography using a Superdex 75 column equilibrated with 0.01 M phosphate, and drugs were used as received. Experiments were carried out using double distilled, deionized, and degassed water. The buffer solutions used was glycine–HCl ( $I = 0.01$  M) for pH 3.0 and sodium monophosphate–sodium diphosphate for pH 7.4 ( $I = 0.01$  M), respectively. HSA was dissolved in each buffer solution and dialyzed extensively against the proper buffer. Protein concentration was determined spectrophotometrically, using a molar absorption coefficient of  $35\,219\text{ M}^{-1}\text{ cm}^{-1}$  at  $280\text{ nm}$ .<sup>19</sup>

**Isothermal Titration Calorimetry (ITC).** Heats of interaction were measured using a VP-ITC titration microcalorimeter (MicroCal Inc., Northampton, MA). In ITC experiments, one measures directly the energy (enthalpy changes) associated with processes occurring at constant temperature, in our case  $25\text{ }^{\circ}\text{C}$ . The titrant and sample solutions were made from the same stock buffer solution, and both experimental solutions were degassed before each titration. The solution in the cell was stirred by the syringe at  $300\text{ rpm}$ , which ensured rapid mixing but did not cause foaming on the protein solution. Typically, small aliquots of a phenothiazine stock solution at a concentration below its critical micelle concentration were injected under automatic control into a known volume (ca.  $1.436\text{ mL}$ ) of a  $0.03\text{ mM}$  HSA aqueous buffered solution held in the calorimeter cell. Repeated additions of the stock drug solution gave the heat evolved ( $Q$ ) as a function of phenothiazine concentration. The volume of each injection was  $8\text{ }\mu\text{L}$ , and the intervals between injections were  $400\text{ s}$  to allow correct equilibration. To correct for the dilution effect by the injection of drug solution, two controls were obtained: titration of HSA solution by the buffer to account for HSA dilution and titration of buffer solution by phenothiazine solution

to account for drug dilution effect. The heats of dilution were, therefore, subtracted from experimental drug onto protein titrations, although this resulted in small heats. The overflow of the reaction mixture by injection of ligand solution, which changes slightly the protein concentration along an experiment, was corrected by the computer. Experiments were repeat two or more times to get a reproducibility of better than 3%.

The direct analysis of ITC data curves for drug binding to HSA allowed the determination of the binding enthalpy ( $\Delta H_{\text{ITC}}^i$ ) and entropy change ( $\Delta S_{\text{ITC}}^i$ ) of drug binding and the apparent binding constants ( $K_{\text{ITC}}^i$ ) with the number of binding sites ( $n_i$ ) in the  $i$ th class of binding site, as follows

$$Q(i) = M_t V_0 \sum_{i=1}^m n_i \theta_i \Delta H_{\text{ITC}}^i \quad (1)$$

where  $Q(i)$  is the heat evolved after the  $i$ th injection,  $M_t$  the total concentration of the protein,  $V_0$  the active cell volume, and  $\theta_i$  the fraction of sites occupied by the phenothiazine. However, the parameter of interest for comparison with experiment is the change in heat content from the completion of the  $i - 1$  injection to completion of the  $i$  injection. Therefore, after completing an injection, it is necessary to make a correction for displaced volume. The correct expression then for heat released,  $\Delta Q(i)$ , from the  $i$ th injection is

$$\Delta Q(i) = Q(i) + \frac{dV_i}{V_0} \left[ \frac{Q(i) + Q(i-1)}{2} \right] - Q(i-1) \quad (2)$$

The data were first analyzed with either availability of one or two binding sites by the Windows-based Origin software package supplied by MicroCal. After subtraction of the heat of dilution, a nonlinear least-squares algorithm and the concentrations of the titrant and sample were used to fit (minimization of  $\chi^2$ ) the heat flow per aliquot, providing best fit values of the stoichiometry ( $n_i$ ), changes in enthalpy ( $\Delta H_{\text{ITC}}^i$ ), entropy ( $\Delta S_{\text{ITC}}^i$ ), and binding constants ( $K_{\text{ITC}}^i$ ).

**Electrophoretic Mobility.**  $\zeta$ -Potentials of the HSA–fluphenazine complexes were measured using a Zetamaster 5002 (Malvern Instruments Ltd) by taking the average of five measurements at stationary level. The cell used was a  $5\text{ mm} \times 2\text{ mm}$  rectangular quartz capillary. The temperature of the experiments was  $25.0 \pm 0.1\text{ }^{\circ}\text{C}$  controlled by a HETO proportional temperature controller. The  $\zeta$ -potential was calculated from the electrophoretic mobility,  $u$ , assuming a protein radius,  $a$ , of approximately  $3.0\text{ nm}$ ,<sup>20</sup> using the relationship<sup>21</sup>

$$\zeta = \frac{3\eta u}{2\epsilon_0 \epsilon_r f(\kappa a)} \quad (3)$$

where the permittivity of vacuum,  $\epsilon_0$ , the relative permittivity of the medium,  $\epsilon_r$ , and the viscosity of water,  $\eta$ , were taken as  $8.854 \times 10^{-4}\text{ J}^{-1}\text{ C}^2\text{ m}^{-1}$ ,  $78.5$ , and  $8.904 \times 10^{-4}\text{ N m}^{-2}\text{ s}$ , respectively. The factor  $f(\kappa a)$  depends on the particle shape; for a sphere with  $\kappa a > 1$  it is given by<sup>22</sup>

$$f(\kappa a) = \frac{3}{2} - \frac{9}{2\kappa a} + \frac{75}{2\kappa^2 a^2} - \frac{330}{\kappa^3 a^3} \quad (4)$$

$\kappa$  being the reciprocal Debye length. In our case, the product  $\kappa a$  was  $3.55$ , corresponding to a Henry factor  $f(\kappa a)$  of  $1.11$ .

**UV–Vis Spectroscopy.** Absorbance spectra were measured using a Beckman spectrophotometer (model DU 640), with six microcuvettes, operating in the UV–visible region. For absorbance spectra, five of the six microcuvettes were filled with protein/drug solutions; the remaining microcuvette contained only buffer and was used as a blank reference. The microcuvettes were filled and placed in the same orientation for all tests. Absorbance was measured at  $25\text{ }^{\circ}\text{C}$  using a temperature controller (Beckman DU series), based on the Peltier effect. For difference spectra values, contributions from both drug-only and protein-only solutions were subtracted.

**Dynamic Light Scattering (DLS).** Dynamic light-scattering measurements were made at  $25.0 \pm 0.1$  °C and at a scattering angle of  $\theta = 90^\circ$  to the incident beam, using an ALV 5000 laser light-scattering instrument equipped with a 500 mW solid-state laser (Coherent Innova) with vertically polarized incident light of wavelength  $\lambda = 532$  nm in combination with a ALV SP-86 digital correlator with a sampling time range of 25–40 ms. All solutions were filtered through a Millipore filter with a  $0.22 \mu\text{m}$  pore size and thermostated the desired temperature for at least 30 min. Experiment duration was in the range of 5–10 min, and each experiment was repeated two or more times.

The correlation functions were analyzed by the constrained regularized CONTIN method to obtain distribution decay rates ( $\tau$ ). The decay rates gave the distribution of the apparent diffusion coefficient

$$D_{\text{app}} = \frac{\tau}{q^2} \quad (5)$$

with the scattering vector,  $q$ ,

$$q = \frac{4\pi n}{\lambda} \sin \frac{\theta}{2} \quad (6)$$

$n$  being the refractive index of water. The apparent hydrodynamic radius,  $r_{\text{app,h}}$ , can be calculated via the Stokes–Einstein equation assuming a spherical geometry

$$r_{\text{app,h}} = \frac{kT}{6\pi\eta D_{\text{app}}} \quad (7)$$

where  $k$  is the Boltzmann constant and  $\eta$  the viscosity of water at temperature  $T$ .

## Results and Discussion

The HSA molecule is known to undergo several well-organized changes in its conformation, usually under nonphysiological conditions: (a) the N–F transition between pH 5.0 and 3.5, involving the unfolding and separation of domain III without significantly affecting the rest of the protein molecule;<sup>23–24</sup> the F form being characterized by a dramatic increase in viscosity, lower solubility, and a significant loss in helical content;<sup>25</sup> (b) the F–E transition between pH 3.5 and 1.2, which is accompanied by a further protein expansion with the loss of the intradomain helices of domain I, which are connected to helices of domain II, and these helices in domain III (In addition, the E form involves an increase in protein intrinsic viscosity and a rise in the hydrodynamic axial ratio from about 4 to 9.<sup>26</sup>); (c) the N–B transition between pH 7.0 and 9.0, where a slight reduction in helical content affecting the two interdomain helices and a small increase in sheet structure occurs;<sup>29</sup> (d) in the presence of denaturant agent, such as urea, HSA showed a two-step three-state transition with an intermediate (I) characterized by unfolding of domain III and partial but significant loss of native conformation of domain I.<sup>27</sup>

In order to study and discriminate the role of the different interactions in the complexation mechanism and affinity, we have performed all experiments at two different pH, 3.0 and 7.4 (the isoelectric point of HSA is 4.9),<sup>28</sup> bearing in mind that the protein conformation at acidic pH is more expanded than at the physiological one, as previously mentioned. In addition, although blood pH is generally stable, there is a pH difference among blood, cerebral blood flow, and intracellular and extracellular environments where ligand–HSA binding occurs, thus affecting drug–HSA interactions.<sup>29</sup>

**Thermodynamics of Complexation.** To directly quantify the energetics of the binding process of fluphenazine onto HSA,

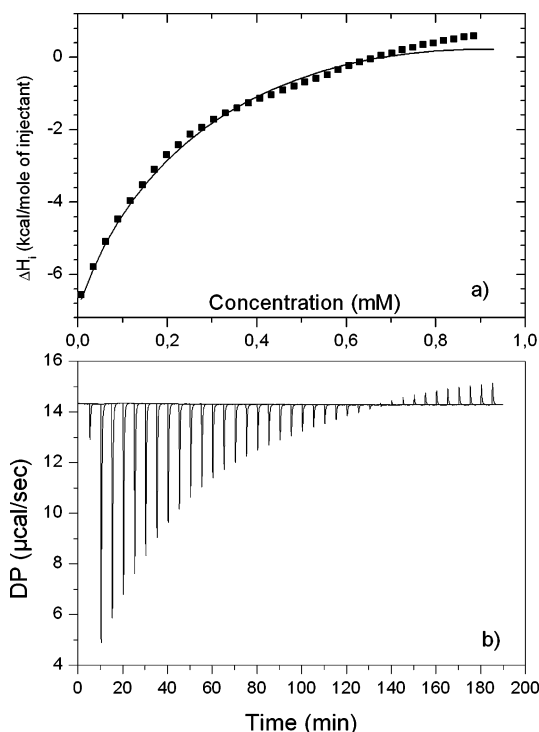


**Figure 1.** (a) Enthalpy of interaction,  $\Delta H^\circ$ , of fluphenazine hydrochloride (5 mM) with 0.03 mM HSA at pH 7.4 and 25 °C. (b) Raw ITC of titration of fluphenazine onto HSA.

**Table 1.** Enthalpy,  $\Delta H^\circ_{\text{ITC}}$ , Entropy,  $\Delta S^\circ_{\text{ITC}}$ , Gibbs Energy,  $\Delta G^\circ_{\text{ITC}}$ , Binding Constant,  $K'_{\text{ITC}}$ , and Number of Binding Sites,  $n_i$ , in HSA Aqueous Buffered Solutions of pH 3.0 and 7.4 at 25 °C for Fluphenazine Hydrochloride<sup>a</sup>

pH	$\Delta H^\circ_{\text{ITC}}$ (kJ mol <sup>-1</sup> )	$T\Delta S^\circ_{\text{ITC}}$ (kJ mol <sup>-1</sup> )	$\Delta G^\circ_{\text{ITC}}$ (kJ mol <sup>-1</sup> )	$10^{-4} K'_{\text{ITC}}$ (M <sup>-1</sup> )	$n_i$
3.0	$-3.2 \pm 0.2$	$20.3 \pm 2.5$	$-23.5 \pm 2.3$	$3.1 \pm 0.1$	$1.6 \pm 0.28$
	$-1.3 \pm 0.3$	$17.5 \pm 1.9$	$-18.8 \pm 1.6$	$0.2 \pm 0.02$	$5.4 \pm 0.33$
7.4	$-29.2 \pm 1.3$	$4.2 \pm 5.2$	$-33.4 \pm 3.9$	$72 \pm 1.0$	$6.1 \pm 0.51$
	$-1.8 \pm 0.2$	$26.2 \pm 2.9$	$-28.0 \pm 2.7$	$4.2 \pm 0.3$	$16.1 \pm 1.32$

<sup>a</sup> First values correspond to the first class ( $i = 1$ ) and second to the second class of binding sites ( $i = 2$ ).

the enthalpies of interaction of the drug with HSA were measured by isothermal titration calorimetry. Figure 1 shows the ITC titration data of a concentration of 0.03 mM HSA by 5 mM of fluphenazine at pH 7.4 and ionic strength of 0.01 M. A similar plot was obtained at pH 3.0 (not shown). Measurements were made at concentrations below the critical aggregation concentration of the drug to eliminate the heat involved in aggregate breakdown due to dilution of a micellar drug stock solution. As commented before, ITC data were fitted by using the Origin software supplied with proper fitting models. Fits to a two-site model provided the best results. Derived values of  $n_i$ ,  $\Delta H^\circ_{\text{ITC}}$ ,  $K'_{\text{ITC}}$ ,  $\Delta S^\circ_{\text{ITC}}$  are shown in Table 1. The obtained results allow us to draw certain conclusions relative to the nature of the molecular interactions involved in the binding and subsequent complex formation. It can be observed that, at physiological pH, the binding affinity increases. This fact originates due to protein and drug differing in the sign of their net electrical charge (negative for HSA and positive for the phenothiazine), thus, in principle, allowing electrostatic interactions between drug molecules and the amino acid residues of the protein. This is reflected in the high negative values of enthalpy of binding,  $\Delta H^\circ_{\text{ITC}}$ , and in a larger affinity binding constant,  $K'_{\text{ITC}}$ , at this pH for the first class of binding sites. The two electric charges presented in the piperazine ring of the



molecular structure of this drug seem, thus, to increase the binding affinity of this phenothiazine to HSA. In this regard, it has been shown that phenothiazine drugs with piperazine rings as lateral chain groups in their molecular structure displayed an enhanced activity, which is directly related to their structure conformation and binding affinity.<sup>30</sup> To confirm the existence of electrostatic interactions, a titration of phenothiazine onto HSA solution of higher ionic strength (0.3 M) showed both an increase (less negative) in  $\Delta H^{\text{ITC}}$  and a decrease of  $K^{\text{ITC}}$ , consistent with the screening of electrostatic interactions. The large negative values of  $\Delta H^{\text{ITC}}$  suggest a possible contribution to this quantity from the formation of new hydrogen bonds (between drug molecules and HSA and/or water–HSA molecules). In this respect, it is known that hydrogen bond formation is always accompanied by heat evolution, with energies lying within  $-7$  to  $-85$  kJ mol<sup>-1</sup>, which comprises the  $\Delta H^{\text{ITC}}$  values obtained at this pH.<sup>31</sup>

At pH 3.0, both protein and drug presents the same sign in their net electrical charge, so binding might only proceed, at first, via hydrophobic interactions. Nevertheless, the expanded state of the HSA molecule at this pH can make accessible some previously buried ionic amino acid residues, enabling some type of electrostatic interaction, as reflected the negative values of  $\Delta H^{\text{ITC}}$  at this pH, since it is known that hydrophobic interactions are endothermic, with energies lying in the range 0.5–3 kJ mol<sup>-1</sup>. This expanded state can also facilitate hydrophobic interactions as a consequence of a better accessibility for the hydrophobic group of the drug molecule to interact through hydrophobic bonding with the nonpolar parts of the protein surface and, overall, within the remaining hydrophobic cavities of the protein molecules. Hydrophobic interactions are playing a key role at this pH, since the binding enthalpy is not highly negative, with the affinity constant,  $K^{\text{ITC}}$ , and the number of drug molecules per binding site sensibly decreasing with respect to pH 7.4, which indicates a reduction in the binding strength. Nevertheless, although hydrophobic interactions are also present at physiological pH in binding to the first class of binding sites, as supported by the positive entropy changes at complex formation,  $\Delta S^{\text{ITC}}$  (see Table 1), and provided that both hydrogen bonds and electrostatic interactions if completely predominant would be accompanied by an entropy decrease,<sup>30</sup> the enthalpic contribution at this pH for these sites seems to be predominant, in agreement with other reports.<sup>32</sup> However, other works have pointed out that the role of electrostatic and hydrogen bonds is almost negligible.<sup>33–36</sup> On the other hand, the Gibbs energies of binding,  $\Delta G^{\text{ITC}}$ , for the second class of binding sites are effectively dominated by large increases in entropy consistent with hydrophobic interactions at both pH. In all cases, the binding process would be spontaneous, as indicated by the negative values of  $\Delta G^{\text{ITC}}$ . In addition,  $\Delta H^{\text{ITC}}$  is more negative than  $\Delta H^{\text{ITC}}$ , indicating that binding to class-one sites would correspond to high-energy sites bound via electrostatic interactions with a larger affinity, whereas class-two sites would involve mainly hydrophobic plus little specific interactions, with lower affinity binding of the drug to the protein. This is in agreement with larger binding constants for first-class binding sites and larger entropy values at complex formation for binding to second-class binding sites, in agreement with previous studies on the binding of amphiphilic drugs to HSA.<sup>35,37</sup> The larger values of  $n_2$  can be related, on one hand, to an expansion of the protein structure induced by drug binding to primary binding sites, which contributes to the increase in the number of available binding sites, allowing a major space in the interior of the protein to accommodate phenothiazine molecules. This behavior results

in an increase of the complex size, as shown by dynamic light scattering next, and even leading to the possible formation of clusters of drug along the HSA molecule.<sup>35</sup>

On the other hand, another contribution to the sensible large number of second-class binding sites for this drug can be also a result of a distortion of the fit in such a region of the plot due to the beginning of complex association, as showed by the positive  $\Delta H^{\text{ITC}}$  values at the highest drug concentrations, which lie in the range of values of hydrophobic interactions. We hypothesize that drug complexation involves a certain neutralization of the net protein charge, which joined to the protein conformational change might involve an increase in the hydrophobicity of the complex, to minimize the free energy of solution, and an aggregation process between complexes should begin, as shown by dynamic light scattering (DLS) in a next section. Besides that, a contribution from the formation of drug aggregates would be also involved in the  $\Delta H^{\text{ITC}}$  values at these drug concentrations, as shown also below, which also affects the data fit. We have also checked the possibility of some precipitation occurring during the experiments. However, no precipitation was observed in solutions even after several weeks.

The concentration of free and bound drug can be calculated by following the treatment of ITC data developed by Ueda and Yamana,<sup>18</sup> which considers a system composed of a solution of  $n_{\text{M}}^{\text{T}}$  moles of protein M and  $n_{\text{X}}^{\text{T}}$  moles of drug X dissolved in  $n_{\text{W}}$  moles of solvent W. Provided that the protein molecule has  $q$  sites, each capable of combining with the drug molecule, then  $q$  species of protein–drug complex  $\text{MX}_i$  ( $i = 1, 2, \dots, q$ ) are formed in the solution. With their model, Ueda and Yamaka obtain the expression for the average number of drug molecules bound to a protein molecule as

$$b = \frac{h^{\text{diff}} - \alpha_{\text{X}}^{\text{T}} h_{\text{X}}}{\Delta h} \quad (8)$$

where  $h^{\text{diff}}$  is the enthalpy difference per mole of protein,  $\alpha_{\text{X}}^{\text{T}} = n_{\text{X}}^{\text{T}}/n_{\text{M}}^{\text{T}}$  the molar ratio of total drug molecules to total protein molecules,  $h_{\text{X}}$  the partial molar enthalpy of the free drug, and  $\Delta h$  the averaged partial molar enthalpy change of the complex formation per drug molecule defined by

$$\Delta h = \frac{\sum_{i=0}^q n_i (h_i - h_0 - i h_{\text{X}})}{\sum_{i=0}^q i n_i} \quad (9)$$

where  $n_i$  and  $h_i$  are the number of moles and the partial molar enthalpy of the free protein ( $i = 0$ ) and of the complex ( $i = 1, 2, \dots, q$ ).

From the initial slope of the curve at low drug concentration and from the final slope of the curve at high concentration, the number of bound and free drug molecules at each injection was obtained. Figure 2 shows the binding isotherms made from the free and bound phenothiazine concentrations for fluphenazine at the different pH. The present study showed that the binding was saturable in the concentration range analyzed conforming Langmuir adsorption isotherms, which are interfacial.

By fitting bound,  $b$ , and free,  $C_{\text{X}}$ , drug molecules to the Scatchard plot, the affinity constants and binding numbers of fluphenazine to HSA can also be calculated.<sup>38</sup> Scatchard plots were nonlinear (see Figure 3), indicating multiple classes of binding sites, in agreement with the results obtained by ITC. Because of the difficulty of identifying intermediate classes of

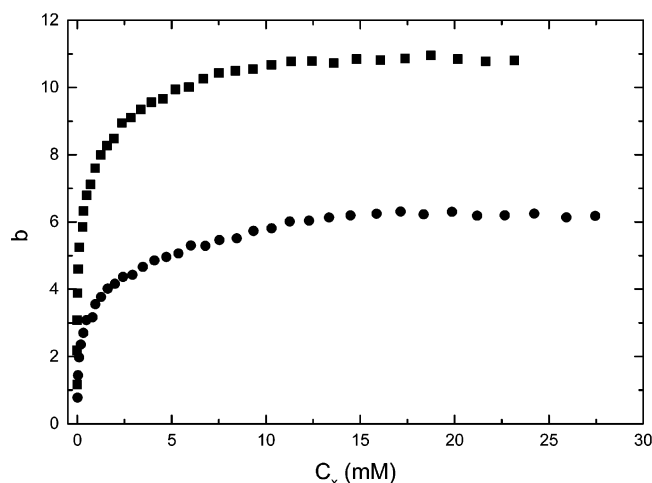


**Figure 2.** Number of bound,  $b$ , and free,  $C_x$ , fluphenazine molecules in a HSA solution of 0.03 mM at (●) pH 3.0 and (■) pH 7.4 at 25 °C.

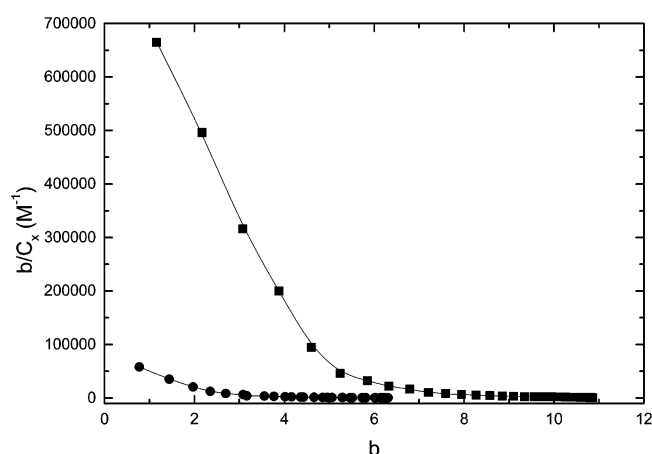


**Figure 3.** Scatchard plots of fluphenazine hydrochloride in the presence of 0.03 mM of HSA at (●) pH 3.0 and (■) pH 7.4 at 25 °C.

**Table 2.** Binding Constants,  $K^i$ , and Number of Binding Sites,  $n_i$ , Obtained from Scatchard Plots

pH	$10^{-4} K^1$	$10^{-3} K^2$	$n_1$	$n_2$
3.0	$2.8 \pm 0.2$	$1.3 \pm 0.1$	$2.7 \pm 0.2$	$6.3 \pm 0.2$
7.4	$17.1 \pm 0.5$	$5.3 \pm 0.3$	$5.5 \pm 0.4$	$11.0 \pm 0.5$

binding, the high-affinity and low-affinity binding classes were analyzed as previously: the high-affinity interaction was estimate at the lowest drug/protein molar ratio, whereas the low-affinity interaction was estimated at the highest drug/protein molar ratios. The results obtained for  $K^i$  and  $n_i$  are shown in Table 2. Differences in the  $K^i$  and  $n_i$  values from Tables 1 and 2 arises from assumptions made in the calculations and different choices of plotting equations, but there is still an acceptable agreement.

**Electrokinetic Behavior of Complexes.** Figure 4 shows the  $\zeta$ -potentials of HSA–fluphenazine complexes in the presence of different concentrations of this drug at different pH. For fluphenazine at pH 3.0, positive  $\zeta$ -potentials are observed as a consequence of the protein being below its isoelectric point. As drug concentration increases,  $\zeta$ -potentials slightly increase, suggesting the adsorption of the positively charged drug on the hydrophobic patches of the protein molecules. However, it is necessary to remark that, at low drug concentrations, there is an interval where  $\zeta$ -potential slightly decreases. This has been thought to result from counterions and some drug monomer adsorption present in the electric double layer of the protein as

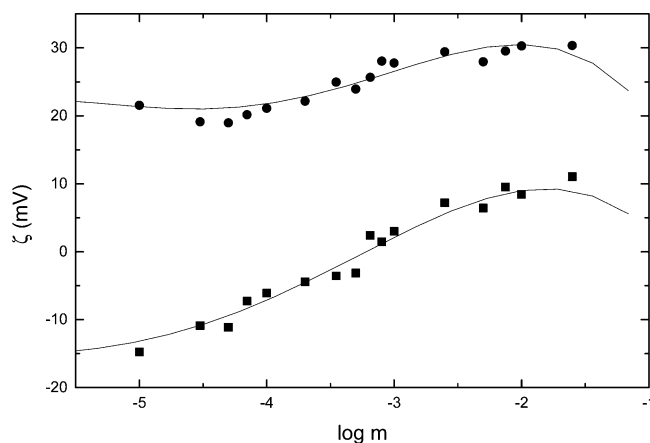


**Figure 4.**  $\zeta$ -Potential data of fluphenazine hydrochloride in the presence of 0.03 mM of HSA at (■) pH 7.4 and (●) pH 3.0 at 25 °C.

a consequence of the more extended conformation of HSA at acidic pH, which can provide accessibility to previously buried electrically charged amino acid residues.<sup>39–40</sup> On the other hand, at pH 7.4 the  $\zeta$ -potential of complexes is negative and, as binding of the drug to protein proceeds, a reversal in the sign of this quantity occurs. In this case, the initial binding of drug monomers seems to take first place via electrostatic interactions to the ionic sites of the protein molecules because macromolecule and drug differ in the sign of their net electric charge. Once the specific binding sites are saturated, an additional hydrophobic adsorption is probably produced onto the hydrophobic cavities of the protein molecules with a certain expansion of complex structure (as shown below), becoming hydrophobic interactions, the main force behind complexation. A similar electrokinetic behavior has been found for other tricyclic amphiphilic drugs, such as the antidepressants clomipramine, imipramine, and nortriptyline.<sup>40–42</sup>

In order to calculate the total number of adsorption sites per unit area on the protein,  $N_1$ , and the complexation constant,  $k_2$ , the Ottewill and Watanabe model (OW)<sup>43–44</sup> was considered

$$-\Delta\sigma_d = \Delta\sigma_i = \frac{(k_1 c)}{1 + (k_2 c)} \quad (10)$$

where  $\Delta\sigma_i$  and  $\Delta\sigma_d$  are the differences between the charge densities on the ion and on the diffuse layer before and after adsorption, respectively, and  $k_1 = zeN_1k_2$ , in which  $z$  is the charge of the adsorbing ions. Assuming that the complex has a spherical form with radius  $a$  and making use of the Debye–Hückel approximation for the solution of the Poisson–Boltzmann (PB) as a first approximation, the change in diffuse layer charge,  $\Delta Q$ , can be related to the change in potential,  $\Delta\Psi_d$ , as follows:<sup>45</sup>

$$-\Delta\sigma_d = \frac{\Delta Q}{4\pi a^2} = \frac{\epsilon_0 \epsilon_r (1 + \kappa a) \Delta\Psi_d}{a} \quad (11)$$

Assuming that  $\Delta\Psi_d = \Delta\zeta$  and by making different substitutions, the change in  $\zeta$ -potential with concentration  $m$  can be expressed as a quadratic expression

$$sm^2k_2^2 + Bk_2 + s = 0 \quad (12)$$

where  $s = d\zeta/dm$ ,  $B = (2sm - Am)$ , and  $A = -((eN_1a)/(\epsilon_0\epsilon_r(1 + \kappa a)))$ . It should be noted that the complexation constant  $k_2$  is only a constant for the formation of a specific complex, i.e., HSA plus a given number of drug molecules.

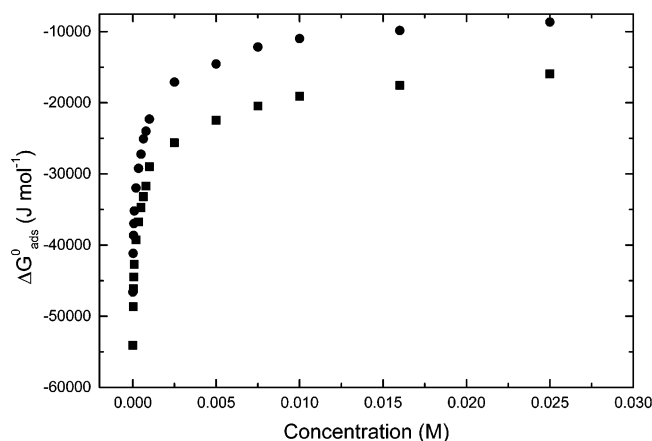


**Figure 5.** Gibbs energy of adsorption,  $\Delta G_{\text{ads}}^{\circ}$ , of fluphenazine hydrochloride in the presence of 0.03 mM HSA at (■) pH 7.4 and (●) pH 3.0 and 25 °C.

**Table 3.** Estimates of the Number of Binding Sites Per Unit Area of Protein Surface,  $N_1$ , and Parameters Characterizing the Drug-Induced Unfolding of HSA (0.03 mM) in Aqueous Buffered Solution of pH 3.0 and 7.4 at 25 °C

pH	$10^{-17} N_1$ ( $\text{m}^{-2}$ )	$\Delta G_{\text{w}}^{\circ}$ ( $\text{kJ mol}^{-1}$ )	$m$ ( $\text{kJ mol}^{-1}$ )	$\nu$	$\ln K$	$\Delta G_{\text{pc}}^{\circ}$ ( $\text{kJ mol}^{-1}$ )	$\Delta(\Delta_r G^{\circ})$ ( $\text{kJ mol}^{-1}$ )
3.0	0.5	12.6	107	2	24.5	-60.7	-73.3
7.4	1.7	10.6	156	4	34.0	-84.2	-94.8

The standard free energy of adsorption,  $\Delta G_{\text{ads}}^{\circ}$ , may be obtained from  $k_2$  using the relationship

$$k_2 = \exp(-\Delta G_{\text{ads}}^{\circ}/kT) \quad (13)$$

As binding proceeds,  $k_2$  and  $\Delta G_{\text{ads}}^{\circ}$  change with the number of bound molecules due to the effect of the already bound drug molecules on further binding. To apply the treatment described above, it is necessary to have a value for  $A$  as well as values of  $s$  as a function of free drug concentration to solve eq 12 for  $k_2$ . The values of  $s$  were obtained by fitting the  $\zeta$ -potential data to polynomials that were differentiated to obtain  $s$  at the required concentrations of phenothiazine. To calculate  $A$ , estimates of  $N_1$  are required. To obtain these values, we assume that the volume of the HSA unit cell<sup>15</sup> is  $0.137 \times 10^{-24} \text{ m}^3$ ; if this volume corresponds to a sphere, its radius would be 3.2 nm, in very good agreement with experimental results,<sup>12</sup> and its surface area would be  $1.29 \times 10^{-16}$ . From this surface area and the total number of binding sites taken from ITC, estimates of the number of sites per unit area were made and are given in Table 3. These values are in close agreement with those obtained for other drug–protein complexes.<sup>40–42,46,47</sup>

Representative plots of the standard Gibbs energies of adsorption from the  $\zeta$ -potential measurements are shown in Figure 5 for fluphenazine.  $\Delta G_{\text{ads}}^{\circ}$  values evaluated from  $\zeta$ -potential data are large and negative at low drug concentrations when specific binding takes place, mainly at pH 7.4 when the protein is negatively charged; at higher drug concentrations,  $\Delta G_{\text{ads}}^{\circ}$  becomes less negative as more drug molecules might bind, leading to an almost constant value of  $\Delta G_{\text{ads}}^{\circ}$ , which suggests a saturation process. A similar behavior has been also noted for other drugs, for example, penicillins and antidepressants and human serum albumin,<sup>40,41,46</sup> in agreement with ITC data.

**Dynamic Light Scattering.** It has been previously argued that an expansion of the protein is the origin of the increase in the number of second-class binding sites,  $n_2$ . In order to check

this point, we have performed dynamic light scattering measurements to determine the size of the protein–drug complexes. Figure 6 shows selected intensity–decay time distributions of the fluphenazine–HSA system at pH 7.4, as an example. Similar distributions were obtained at pH 3.0 (not shown). The distributions obtained at very low drug concentration ( $1 \times 10^{-5}$ – $5 \times 10^{-4} \text{ M}$ ) did not involve any appreciable change in the time distribution upon binding. However, at higher drug concentrations ( $5 \times 10^{-4}$ – $2.5 \times 10^{-2} \text{ M}$ ) a broadening and shift to higher decay time occurs, which may be related to an increase in the size of the complex and to certain polydispersity. It is worth mentioning that this broadening is less intense at pH 3.0 as a consequence of the already expanded state of HSA and the lesser binding at the latter pH.

In addition, an additional peak at fast decay time ( $\sim 0.005 \text{ ms}$ ) appears at 0.0075 M as a consequence of the existence of some drug aggregates with a size of 0.8–1.0 nm starting to form in solution at a concentration where free-only drug molecules in solution do not associate.<sup>47</sup> Thus, the presence of protein molecules in solution seems to be the origin of this preaggregation of the phenothiazine in a similar manner as some tricyclic antidepressants<sup>42–43</sup> and the well-studied phenomenon of polymer-induced aggregation of classical surfactants.<sup>48</sup> Also, a third peak at very large decay time ( $\sim 2 \text{ ms}$ ) also is present, which can be assigned to the formation of a small fraction of clusters with a size of 40–50 nm formed from the association of protein complexes as a consequence of a loss of the protein conformational structure. Complex association has been also noted for other related systems, such as SDS/BSA<sup>20</sup> or antidepressant/HSA systems.<sup>42,43</sup> Despite the amount of scattered light being appreciable, the importance of this population is rather small, less than 2% in mass. This is also reflected in the UV–vis section as discussed below. These data also seem to confirm the ITC profile previously described.

Figure 7 shows the corresponding apparent hydrodynamic radii,  $r_{\text{h,app}}$ , of the fluphenazine–HSA complexes plotted as a function of the total drug concentration at pH 3.0 and 7.4, respectively. The total concentration includes both the bound and unbound compound. It is worth mentioning that the hydrodynamic radius of HSA at pH 3.0 is 3.8 nm, in agreement with previous reports,<sup>49,50</sup> and higher than that of pH 7.4 (3.2 nm), as a consequence of the molecular expansion of the protein structure in acidic medium. It is possible to observe in this figure that for both pH values at very low drug concentrations there are no appreciable changes in the size of the complex, in spite of some binding taking place, mainly at pH 7.4. This larger affinity for binding at the latter pH is seen by the earlier increase in the size of the protein–drug complexes ( $\sim 7.5 \times 10^{-5} \text{ M}$ ). As the drug concentration increases, the size of the complex also does (between  $7.5 \times 10^{-5}$  and  $5 \times 10^{-4} \text{ M}$  at pH 7.4 and between  $2 \times 10^{-4}$  and  $7 \times 10^{-4} \text{ M}$  at pH 3.0, respectively), this increment being larger at pH 7.4 and assigned to a further expansion of the protein structure induced by drug binding as a result of protein destabilization (see UV–vis section), as commented previously. Figure 7 might also resemble in some way a typical binding isotherm, which shows the average number of ligand molecules bound per protein molecule as a function of the free ligand in solution. In general, a binding isotherm displays four characteristic regions with increasing ligand concentrations: (a) specific binding, where electrostatic binding occurs (between  $7.5 \times 10^{-5}$  and  $2 \times 10^{-4} \text{ M}$  at pH 7.4 and between  $1 \times 10^{-4}$  and  $3.5 \times 10^{-4} \text{ M}$  at pH 3.0, respectively); (b) noncooperative binding (between 2.0 and  $5.0 \times 10^{-4} \text{ M}$  and 3.5 and  $7.0 \times 10^{-4} \text{ M}$  at pH 7.4 and 3.0,

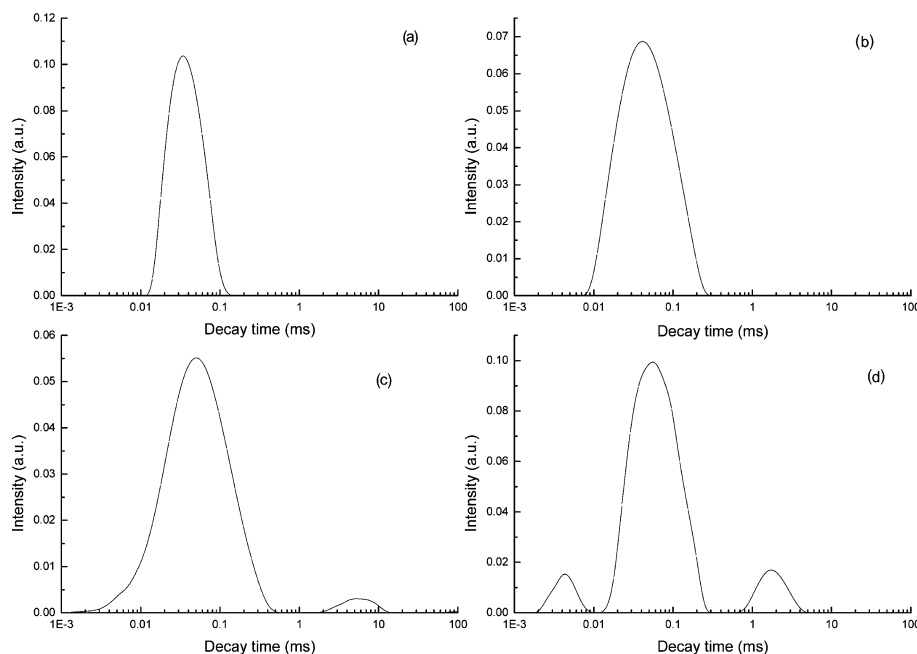


**Figure 6.** Intensity vs decay time distributions of 0.03 mM HSA in the presence of (a)  $5 \times 10^{-5}$ , (b)  $7.5 \times 10^{-4}$ , (c)  $7.5 \times 10^{-3}$ , and (d)  $2.5 \times 10^{-2}$  M of fluphenazine at pH 7.4 and 25 °C.

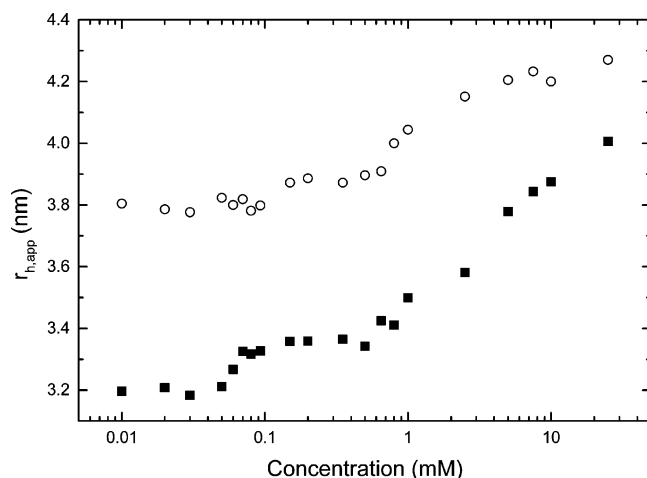


**Figure 7.** Apparent hydrodynamic radii of fluphenazine–HSA complexes at (○) pH 3.0 and (■) pH 7.4 and 25 °C.

respectively (flat region in Figure 7); (c) cooperative binding from  $5 \times 10^{-4}$  M at pH 7.4, for example, where an appreciable increase in complex size occurs as a consequence of further protein expansion; and (d) saturation (not present).

In addition, the expanded protein structure at acidic pH contributes to an enhancement of drug binding as a result of additional hydrophobic bonding to the previously buried non-polar parts of the protein, as observed from the slighter variation of  $r_{h,app}$  with drug concentration at this pH. As the pH rises, the increase in drug binding strength is reflected in a larger variation of the complex radius, where electrostatic interactions are more important, as commented before. Finally, as occurred for tricyclic antidepressants<sup>40–42</sup> and in contrast to anionic amphiphilic drugs such as penicillins,<sup>46</sup> the change in complex size is less dramatic than in the latter case, as a consequence of the minor projection further from the protein surface of the glutamyl and aspartyl side chains, which are involved in the electrostatic binding of cationic compounds, than the arginyl and lysyl side chains involved in anionic drug binding, which allows binding to a greater extent.<sup>46,51</sup>

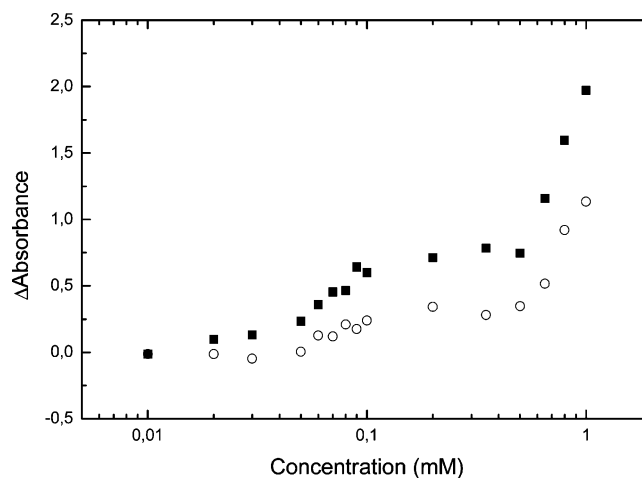


**Figure 8.** Differential absorbance of HSA (0.03 mM) in the presence of fluphenazine hydrochloride at (○) pH 3.0 and (■) pH 7.4 at 25 °C.

**UV–Vis Spectroscopy.** To study the effect of phenothiazine binding on the conformation structure of HSA-absorption spectra of the protein in each medium with different amounts of drug at 298.15 K in the wavelength range 225–500 nm were collected. Figure 8 shows the absorbance changes for the 280 nm difference spectral band of HSA as a function of drug concentration.

At both pH there are two transition regions. The first transition is a change induced by the binding of the drug to the protein involving a conformational change in protein structure, which takes place over a slightly larger drug concentration range at pH 7.4. This is a result of a change in the environment of tryptophan and tyrosine residues upon drug binding, indicating a severe change in the region where these residues are located, pointing out a certain denaturation of the protein molecules.<sup>52</sup> The second transition is a more abrupt change, as denoted by the steep increase in the optical density of the solutions. Additional conformational changes in protein structure should occur, but most important, the formation of drug aggregates and complexes clusters, as seen by DLS, should contribute to this absorbance increase. The complex clusters would be



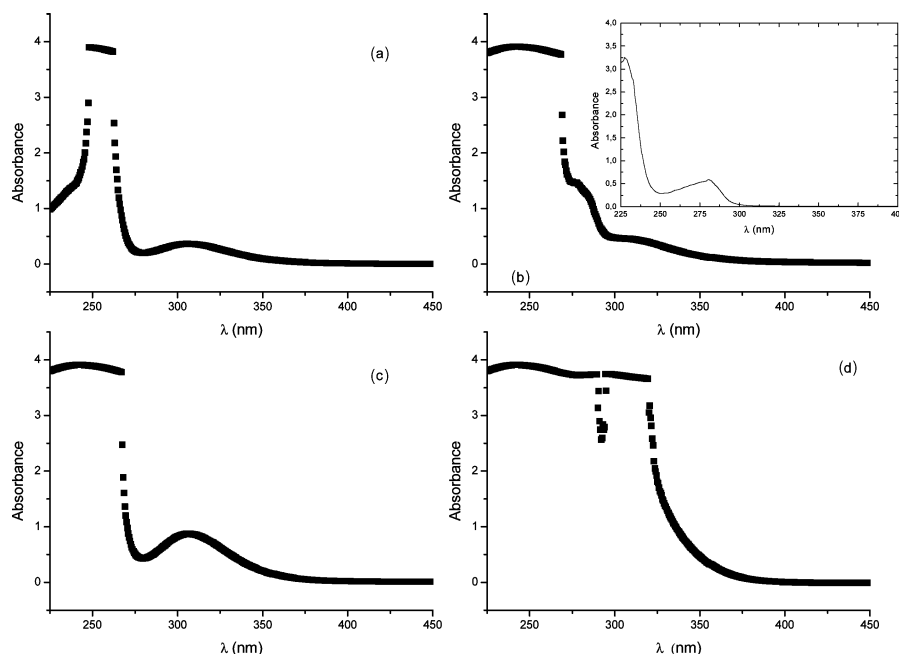


**Figure 9.** Absorbance spectra of (a) HSA–fluphenazine and (b) fluphenazine only solutions with drug concentration 0.1 mM and (c) HSA–fluphenazine and (d) fluphenazine only solution with drug concentration 2 mM. The inset shows the absorbance spectrum of native HSA. In all spectra, HSA concentration is 0.03 mM at pH 7.4 and 25 °C.

probably formed by unfolded protein molecules with attached drug aggregates, resembling the necklace model. These results suggest that the interaction of the drug with HSA undergoes a significant change in its conformation. This can also be seen from Figure 9, where selected absorbance spectra are shown. It can be observed that, as the drug concentration increases, not only an increase in the absorption band at 280 nm occurs but also the development of an additional peak at 320 nm, which cannot be only assigned to drug absorption. This might indicate the formation of drug aggregates onto the protein.

In order to get additional information about the thermodynamics of the protein conformational change, we have tried to analyze the energetics of the first drug-induced transition, as a first approximation, by modeling the interaction between HSA and the drug as a transition between the two macroscopic states: the original state (N) and an altered state with  $\nu$  bound ligand molecules (S)



where  $\nu$  is the average number of drug molecules bound to complex  $DS_{\nu}$ .

We have not modeled the second transition because other phenomena apart from protein denaturation are also included in absorbance data (formation of drug aggregates and protein clusters), altering the meaning of the thermodynamic quantities. The analysis of the equilibrium unfolding transition requires extrapolation of the baseline for the original and altered protein into the transition region to determine the fraction of altered molecules,  $F_D$ , as a function of the unfolding parameters<sup>53</sup>

$$F_D = \frac{A_N - A_{OBS}}{A_N - A_D} \quad (15)$$

where  $A_{OBS}$  is the absorbance observed and  $A_N$  and  $A_D$  are the absorbance for the original and altered conformations, respectively.

The difference in the standard Gibbs energy between the original and altered conformations for the transition can be then calculated as

$$\Delta G^{\circ} = -RT \ln K_D = -RT \ln \left( \frac{A_N - A_{OBS}}{A_{OBS} - A_D} \right) \quad (16)$$

where  $K_D$  is the ratio of altered to original molecules,  $K_D = F_D/(1 - F_D)$ . The equilibrium constant  $K$  for eq 14 is

$$K = \frac{[DS_{\nu}]}{[N][S]^{\nu}} = \frac{K_D}{[S]^{\nu}} = \frac{F_D/(1 - F_D)}{[S]^{\nu}} \quad (17)$$

Figure 10 shows that  $\Delta G^{\circ}$  and  $\ln K_D$  are linear functions of  $[S]$  in a determined range of drug concentrations for a temperature of 25 °C, consistent with the relationships

$$\Delta G^{\circ} = \Delta G_w^{\circ} - m[S] \quad (18)$$

$$\ln K_D = \ln K_w + \frac{m}{RT} \ln[S] \quad (19)$$

where  $\Delta G_w^{\circ}$  is the Gibbs energy at zero concentration of denaturant. Thus, to obtain values of  $\Delta G_w^{\circ}$ , a reliable procedure for the extrapolation of  $\Delta G^{\circ}([S])$  to zero denaturant concentration is required. In this respect, numerous observations of a large number of different proteins showed that, in the transition region, the Gibbs energy of unfolding is, in a relatively narrow range, a linear function of denaturant concentration.<sup>54</sup> This observation led to the so-called linear extrapolation method (LEM). In this method, the so-called denaturant  $m$ -values are a measure of the dependence of  $\Delta G^{\circ}$  on drug concentration,  $[S]$ , and the  $m[S]$  term thus represents the difference in transfer Gibbs energy between the altered and original states. The most attractive feature of this analysis is that it allows us to estimate the stability of a protein over a range of conditions of interest.

The values of  $\Delta G_w^{\circ}$  and  $m$  have been calculated using eqs 18 and 19. These parameters have been both derived from the



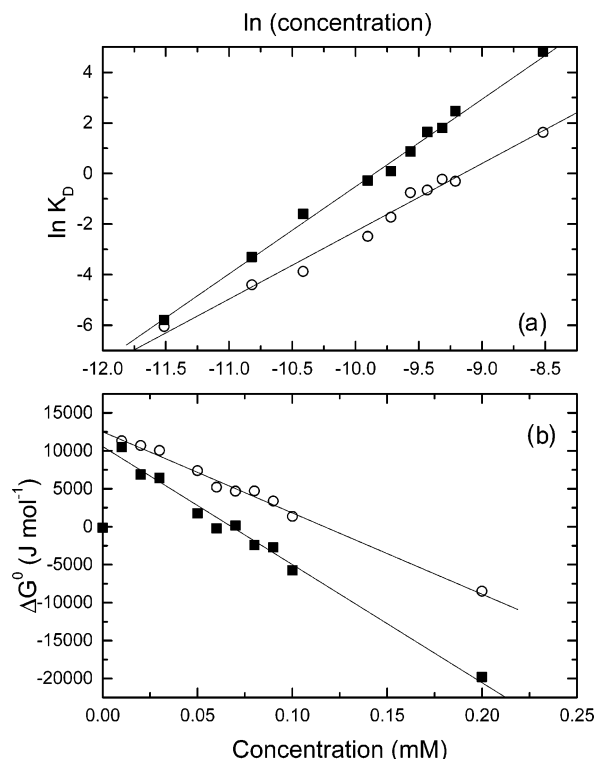


**Figure 10.** (a) Relationship between the logarithm of altered to original molecules ratio for HSA (0.03 mM) in aqueous buffered solutions of fluphenazine hydrochloride at (■) pH 7.4 and (○) pH 3.0. (b) Standard Gibbs energy differences between the folded and unfolded conformations ( $\Delta G^\circ$ ) of HSA (0.03 mM) in aqueous buffered solutions of fluphenazine at (■) pH 7.4 and (●) pH 3.0. The solid line represents eq 19 taking the average parameters given in Table 3.

assumption that  $A_N - A_D$  is constant, i.e.,  $A_N$  and  $A_D$  were taken from the start and finish of the transition. The values are shown in Table 3. From eq 17 and at a drug concentration of 1 mol dm<sup>-3</sup>,  $\ln K = \ln K_D$  and the equilibrium constant  $K$  corresponds to the unfolding transition in a drug-saturated complex in a hydrophobic environment with a Gibbs energy change  $\Delta G_{hc}^\circ$ . Using least-squares analysis of plots of  $\ln K_D$  vs  $\ln[\text{drug}]$  the values of  $\Delta G_{hc}^\circ$  and  $\nu$  were obtained (see Table 3). The difference in Gibbs energies of transfer of the unfolded and native state from water to a hydrophobic environment,  $\Delta G_{hc}^\circ - \Delta G_w^\circ$ , defined as  $\Delta(\Delta_{tr}G^\circ)$ , was also calculated.<sup>55</sup>

The results shown in Table 3 suggest that binding of the drug alters the structural conformation of the protein molecules. Thermodynamic quantities are more negative at pH 7.4 than at pH 3.0, suggesting that, at the former pH, the larger extent of complexation makes the protein structure more accessible to solvent, with a more opened protein structure reflected in larger hydrodynamic radii of protein complexes, as previously commented. The different electrical charge between the protein and drug molecules at pH 7.4 should contribute to a tighter complexation at this pH.  $m$  values show a close dependence on the pH variation of the medium, suggesting that the extent of binding with subsequent protein conformational change depends on the electrical charge of the protein. This is in agreement with the fact that at the isoelectric point the electrostatic interactions are small and, therefore, the free energy of unfolding is due to the solvophobic effect during the denaturation process.<sup>55</sup> Similar results were obtained in the denaturation studies of different proteins, such as bovine catalase<sup>56</sup> or myoglobin<sup>57</sup> and also human serum albumin.<sup>58</sup> On the other hand,  $\nu$  values are in agreement with those corresponding to the stoichiometry of the first class of binding sites derived from ITC data.

## Summary

In the present work, we analyze the complexation process of the phenothiazine drug fluphenazine hydrochloride to HSA in aqueous buffered solutions of pH 3.0, and 7.4, with a view to elucidate the effect of hydrophobic and electrostatic forces on the complexation process and the alteration of protein conformation upon binding. ITC data also show that binding occurs at two different classes of binding sites. It also demonstrates that at acidic pH, hydrophobic interactions between the phenothiazine and the protein play the predominant role in the complexation process, although the existence of electrostatic interactions is also noted. However, at physiological pH, electrostatic interactions and possibly hydrogen-bonding also play an important role for binding to the first class of binding sites, as derived from thermodynamic quantities. In addition, binding to the second class of binding sites at this pH is again dominated by hydrophobic forces, as seen from the entropy increases. This is also pointed out by the small exothermic values of enthalpies of binding, so that the Gibbs energies of binding are dominated by large increases in entropy, consistent with hydrophobic interactions. From ITC data and using a theoretical model, the number of drug molecules adsorbed was derived and, thus, the binding isotherms obtained for both pH values. These isotherms show that binding in the analyzed concentration region is of Langmuir type and saturable. The increase of the hydrodynamic radii obtained from dynamic light scattering with drug concentration indicates an expansion of the protein structure due to drug complexation. At the highest drug concentrations, an association process of protein complexes is detected, possibly resulting in the clustering of drug molecules around the hydrophobic amino acid residues of the unfolded polypeptide chain, which aggregates. In addition, formation of drug aggregates in solution is also noted at concentrations below the critical micelle concentration of the drug.  $\zeta$ -Potential data measurements allow us to calculate Gibbs energies of binding using a modified Ottewill–Watanabe theory. Adsorption Gibbs energies so calculated are of similar magnitude as those obtained from ITC. The process of protein unfolding as a function of added drug has been also monitored by UV–vis spectroscopy. Evidence of complex and drug aggregation is also confirmed. Absorbance data allow us to calculate the Gibbs energy of the transition in water ( $\Delta G_w^\circ$ ) and in a hydrophobic environment ( $\Delta G_{hc}^\circ$ ).

**Acknowledgment.** Authors thank MEC for Research project MAT2004-02756 and Xunta de Galicia for financial support.

## References and Notes

- Benedouch, D.; Chen, S. H. *J. Phys. Chem.* **1983**, *87*, 1473.
- Chakrabarty, A.; Mallick, A.; Haldar, B.; Das, P.; Chattopadhyay, N. *Biomacromolecules* **2007**, *8*, 920.
- Peters, T., Jr. *All about albumin: Biochemistry, genetics and medical application*; Academic Press, Inc.: New York, 1996.
- Kragh-Hansen, U. *Pharmacol. Rev.* **1981**, *33*, 17.
- He, X.; Carter, D. C. *Nature* **1992**, *358*, 209.
- Sneppe, K.; Zocchi, G. *Physics in Molecular Biology*; Cambridge University Press: Cambridge, UK, 2006.
- Zucker, S. D.; Goessling, W.; Gollan, J. L. *J. Biol. Chem.* **1995**, *270*, 1074.
- Ahmad, B.; Parveen, S.; Khan, R. H. *Biomacromolecules* **2006**, *7*, 1350.
- Creighton, T. E. Kim, R. S. *Curr. Opin. Struct. Biol.* **1991**, *1*, 3.
- Attwood, D. *Adv. Colloid Interface Sci.* **1995**, *55*, 271.
- Atherton, A. D.; Barry, B. W. *J. Colloid Interface Sci.* **1985**, *106*, 479.
- Perrine, D. M. In *The Chemistry of Mind-Altering Drugs: History, Pharmacology, and Cultural Context*; American Chemical Society: Washington, DC, 1996.

- (13) Korth, C.; May, B. C.; Cohen, F. E.; Prusiner, S. B. *Proc. Natl. Acad. Sci. U.S.A.* **2001**, 98, 403.
- (14) Mazumder, R.; Ganguly, K.; Dastidar, S. G.; Chakrabarty, A. N. *Int. J. Antimicrob. Agents* **2001**, 18, 403.
- (15) Lind, K. E.; Du, Z.; Fujinaga, K.; Peterlin, B. M.; James, T. L. *Chem. Biol.* **2002**, 9, 185.
- (16) Tsakovska, I. M. *Bioorg. Biomed. Chem.* **2003**, 11, 2889.
- (17) Mayer, M.; James, T. L. *J. Am. Chem. Soc.* **2004**, 126, 4453.
- (18) Ueda, I.; Yamanaka, M. *Biophys. J.* **1997**, 72, 1812.
- (19) Pace, C. N.; Vajdos, F.; Fee, L.; Grimsley, G.; Gray, T. *Protein Sci.* **1995**, 4, 2411.
- (20) Valstar, A.; Brown, W.; Almgren, M. *Langmuir* **1999**, 15, 2366.
- (21) Bier, M. *Electrophoresis. Theory, Methods and Applications*; Academic Press: New York, 1997.
- (22) Hunter, R. J. *Zeta Potential in Colloid Science*; Academic Press: London, 1981; Chapter 3.
- (23) Geisow, M. J.; Beaven, G. H. *Biochem. J.* **1977**, 165, 477.
- (24) Khan, M. Y. *Biochem. J.* **1986**, 236, 307.
- (25) Foster, J. F. In *Plasma Proteins*; Putnam, F. W., Ed.; Academic Press: New York, 1960; Vol. 1.
- (26) Dockal, M.; Carter, D. C.; Ruker, F. J. *Biol. Chem.* **2000**, 275, 3042.
- (27) Ahmad, B.; Khan, M. K. A.M Haq, S.; Khan, R. H. *Biochem. Biophys. Res. Commun.* **2004**, 314, 166.
- (28) Houska, M.; Brynda, E. J. *Colloid Interface Sci.* **1997**, 188, 243.
- (29) Yamasaki, K.; Maruyama, T.; Yoshimoto, K.; et al. *Biochim. Biophys. Acta* **1999**, 1432, 313.
- (30) Feinberg, A. P.; Snyder, S. H. *Proc. Nat. Acad. Sci. U.S.A.* **1975**, 72, 1899.
- (31) Landau, M. A.; Markovich, M. N.; Piruzyan, L. A. *Biochim. Biophys. Acta* **1977**, 493, 1.
- (32) Verbeeck, R. K.; Cardinal, J. A.; Hill, A. G.; Midha, K. K. *Biochem. Pharmacol.* **1983**, 32, 2565.
- (33) Sharples, D. J. *Pharm. Pharmacol.* **1976**, 28, 100.
- (34) Perrin, J. H.; Hulshoff, A. J. *Pharm. Pharmacol.* **1976**, 28, 793.
- (35) Huang, P. C.; Gabay, S. *Biochem. Pharmacol.* **1974**, 9, 175.
- (36) Aki, H.; Yamamoto, M. J. *Pharm. Pharmacol.* **1989**, 41, 674.
- (37) Barbosa, S.; Taboada, P.; Mosquera, V. *Chem. Phys.* **2005**, 310, 51.
- (38) Scatchard, G. *Ann. N.Y. Acad. Sci.* **1949**, 51, 660.
- (39) Sabaté, R.; Estelrich, J. *Int. J. Biol. Macromol.* **2001**, 28, 151.
- (40) Taboada, P.; Gutiérrez-Pichel, M.; Mosquera, V. *Biomacromolecules* **2004**, 5, 1116.
- (41) Taboada, P.; Gutiérrez-Pichel, M.; Barbosa, S.; Mosquera, V. *Phys. Chem. Chem. Phys.* **2004**, 6, 5203.
- (42) Leis, D.; Barbosa, S.; Attwood, D.; Taboada, P.; Mosquera, V. *Langmuir* **2002**, 18, 8178.
- (43) Taboada, P.; Mosquera, V.; Ruso, J. M.; Sarmiento, F.; Jones, M. N. *Langmuir* **2000**, 16, 6795.
- (44) Ottewill, R. H.; Watanabe, A. *Kolloid Z.* **1960**, 170, 132.
- (45) Hunter, R. J. *Zeta Potential in Colloid Science*; Academic Press: London, 1981; Chapter 2.
- (46) Ruso, J. M.; Attwood, D.; García, M.; Taboada, P.; Varela, L. M.; Mosquera, V. *Langmuir* **2001**, 17, 5189.
- (47) Cheema, M. A.; Barbosa, S.; Sidiqq, M.; Taboada, P.; Mosquera, V. *J. Chem. Eng. Data*, submitted.
- (48) Goddard, G. D.; Ananthapadmanaban, K. P. In *Interactions of Surfactant with Polymers and Proteins*; CRC Press: Boca Raton, FL, 1993.
- (49) Taboada, P.; Fernández, Y.; Mosquera, V. *Biomacromolecules* **2004**, 5, 2201.
- (50) Luik, A. I.; Naboka, Y. N.; Mogilevich, S. E.; Huscha, T. O.; Mischenko, N. I. *Spectrochim. Acta Part A*, **1998**, 54, 1503.
- (51) Nozaki, Y.; Reynolds, J. A.; Tanford, C. J. *Biol. Chem.* **1974**, 249, 4452.
- (52) Demchenko, A. P. *Ultraviolet Spectroscopy of Proteins*; Springer-Verlag: Berlin, 1981; Vol. 65, p 427.
- (53) Pace, C. N.; Shirley, B.; Thomson, J. In *Protein Structure and Function: A Practical Approach*; Creighton, T. E., Ed.; IRL: Oxford, 1989; p 311.
- (54) Makhatadze, G. J. *Phys. Chem B* **1999**, 103, 4785.
- (55) Housaindokht, M. R.; Jones, M. N.; Newal, J. F.; Prieto, G.; Sarmiento, F. J. *Chem. Soc. Faraday Trans.* **1993**, 89, 1963.
- (56) Alonso, D. O. V.; Dill, K. A. *Biochemistry* **1991**, 30, 5974.
- (57) Prieto, G.; Suárez, M. J.; González-Pérez, A.; Ruso, J. M.; Sarmiento, F. *Phys. Chem. Chem. Phys.* **2004**, 6, 816.
- (58) Farruggia, B.; Picó, G. A. *Int. J. Biol. Macromol.* **1999**, 26, 317.

BM070354J